5-2011

Persistent Activity in Assortative Networks of Integrate and Fire Neurons

Matthew D. Peppe
College of William and Mary

Persistent Activity in Assortative Networks of Integrate and Fire Neurons

A thesis submitted in partial fulfillment of the requirement
for the degree of Bachelor of Science in Mathematics from
The College of William and Mary

by

Matthew Peppe

Accepted for HONORS

Gregory Smith, Director

Tanujit Dey

Leah Shaw

Junping Shi

Williamsburg, VA
April 27, 2011

Persistent Activity in Assortative Networks of Integrate and Fire Neurons

Matthew D. Peppe

Advisor: Gregory D. Smith

April 27, 2011

Abstract

A neuronal network can be represented as a directed graph. Each neuron corresponds to a node and each connection between the axon of one neuron and the dendrite of another corresponds to an edge. We investigate the effects of two statistical properties of directed graphs on the capacity of excitatory and inhibitory neuronal networks to exhibit bistability. One measure is node-degree correlation, the propensity of nodes to have similar in-degrees and out-degrees. The other measure is edge-degree correlation, the correlation between the in-degree of one node and the out-degree of a node receiving input from the first. By grouping subpopulations of neurons according to their in and out degrees, we perform simulations testing the effect of these different forms of assortativity on network input/output properties. We show that the node-degree correlation and edge-degree correlation of a neuronal network affect the ranges of synaptic coupling strengths and of external stimulation rates for which there are two steady-state mean firing rates. The existence of bistability and hysteresis is important as the physiological basis of short term memory.

Contents

Chapter 1

Introduction

Experimental work shows the neural mechanism behind short term working memory is synaptic reverberation, which refers to activity in excitatory feedback loops that persists in the absence of a stimulus [7]. The neuronal networks underlying this phenomenon must be capable of exhibiting hysteresis. This can be explained by the presence of two stable steady-state firing rates for some levels of external stimulation. Only the single quiescent steady-state exists at low external stimulation rates; the active steady-state alone exists at high stimulation rates. When the external stimulation rate is in the bistable range, the network is quiescent or active depending on whether it had been previously activated or suppressed. Network structure and parameters such as strength of synaptic conductances influence the presence of hysteresis.

Graph theoretical statistical measures of network properties are being applied to problems in neuroscience with growing frequency. According to Olaf Sporns, "The quantitative analysis of neuroanatomical networks can provide important clues for relating anatomical structure to physiological function. Network measures allow the objective characterization of how nodes and edges participate in the overall network" [6]. One such measure is node-degree correlation. Figure 1.1 on the following page provides examples of two small networks with different node-degree correlations. In the correlated network, nodes with

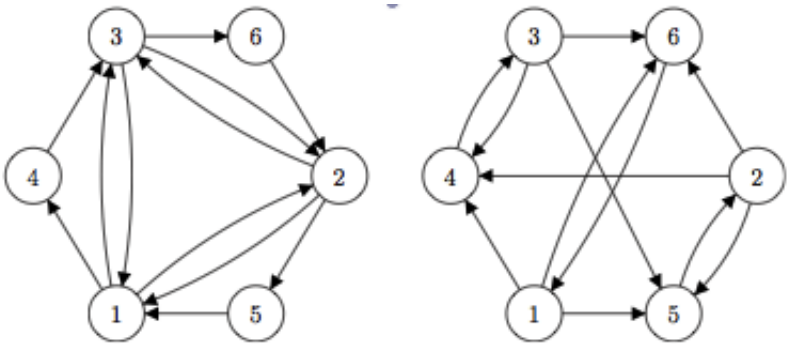

Figure 1.1: Left: A network with positive node-degree correlation ($\rho = 1$)
Right: a network with negative node-degree correlation ($\rho = -1$).
Figure taken from LaMar and Smith (2010) [3].

high in-degree also tend to have high out-degree and nodes with low in-degree tend to have low out-degree. In the anti-correlated network, nodes with high in-degree tend to have low out-degree and vice versa.

Previous work by Smith and Lamar investigated the impact of node-degree correlation on the synchronization of pulse-coupled oscillators [3]. This thesis investigates the node-degree correlation previously studied by Smith and Lamar as well as a related network measure, edge-degree correlation. Instead of studying how these network measures affect synchronization, it investigates how they impact the parameter-dependence of hysteresis. The underlying model is also more physiologically realistic. We use integrate-and-fire neuron models rather than pulse-coupled oscillators. To make the modeling of very large networks of integrate-and-fire neurons computationally feasible we utilize the mean-field limit of a population density model developed by David Cai [1]. Previous work by Shkarayev et. al. (reference [4]) incorporated the in-degree of neurons into this model in order to study the effect of scale-free degree distributions. In order to study the impact of correlations between in and out degrees, we extended the model in such a manner as to allow specification of the joint distribution of in and out degrees.

Chapter 2

Model Formulation

2.1 Networks of Neurons

We model a group of connected neurons as a directed graph. When a neuron fires, it propagates a signal through its axon, which branches and connects to the dendrites of other neurons. The cell voltage of these other neurons changes in response to input received through their dendrites, affecting the rate at which these post-synaptic neurons fire. In the graph representation of a neuronal network, each neuron is represented by a node (or vertex). The connections from axon to dendrite are represented by directed edges. We assume that no neuron has more than 40 presynaptic or postsynaptic neurons within the network.

Directed graphs may display various forms of assortativity. We investigate the effects of two statistical properties of directed graphs. One measure is node-degree correlation, the correlation between the in and out degrees of a node. This is the relationship between i and j (or k and l) in Figure 2.1 on the next page. The other measure is edge-degree correlation, which measures the correlation between the in-degree of a presynaptic neuron and the out-degree of a post-synaptic neuron. This is the relationship between k and j in Figure 2.1 on the following page. Other in and out degree correlations may also have physiologically

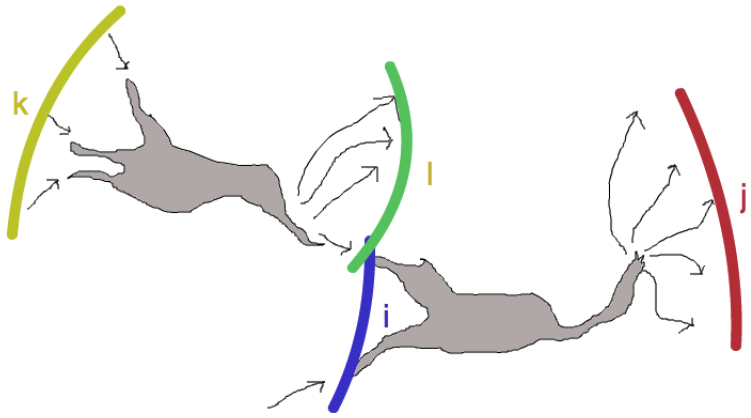

Figure 2.1: Diagram of a pre-synaptic neuron (left) and a post-synaptic neuron (right) where i is the number of incoming connections to a neuron's dendrites, j is the number of outgoing connections from it's axon, k is the number of incoming connections to a presynaptic neuron, and l is the number of outgoing connections from the presynaptic neuron.

relevance but this study does not address them.

For a given network, we measure node and edge-degree correlations using the Pearson's correlation coefficients ρ given in equations 2.1 and 2.2. The sum for ρ_{node} is over all neurons in the network, the sum for ρ_{edge} is over all edges in the network. The mean value of a degree i is written μ^i and its standard deviation as σ^i.

$$\rho_{node} = \frac{1}{N}\sum_{n=1}^{N}(\frac{j_n - \mu^j}{\sigma^j})(\frac{i_n - \mu^i}{\sigma^i}) \tag{2.1}$$

$$\rho_{edge} = \frac{1}{N}\sum_{n=1}^{N}(\frac{j_n - \mu^j}{\sigma^j})(\frac{k_n - \mu^k}{\sigma^k}) \tag{2.2}$$

$P_{node}(i,j)$ is the proportion of neurons in the network with in-degree i and out-degree j. $P_{edge}(k,j)$ is the proportion of edges in the network where the presynaptic node has in-degree k and the post-synaptic neuron has out-degree l. We assume that $1 \leq i,\ j,\ k \leq 40$ and that the marginal degree distributions of i, j, and k are uniform. For any specific values of ρ_{node} and ρ_{edge}, we calculate $P_{node}(i,j)$ and $P_{edge}(k,j)$ using Gaussian copulas as implemented in MATLAB's built-in copulacdf function.

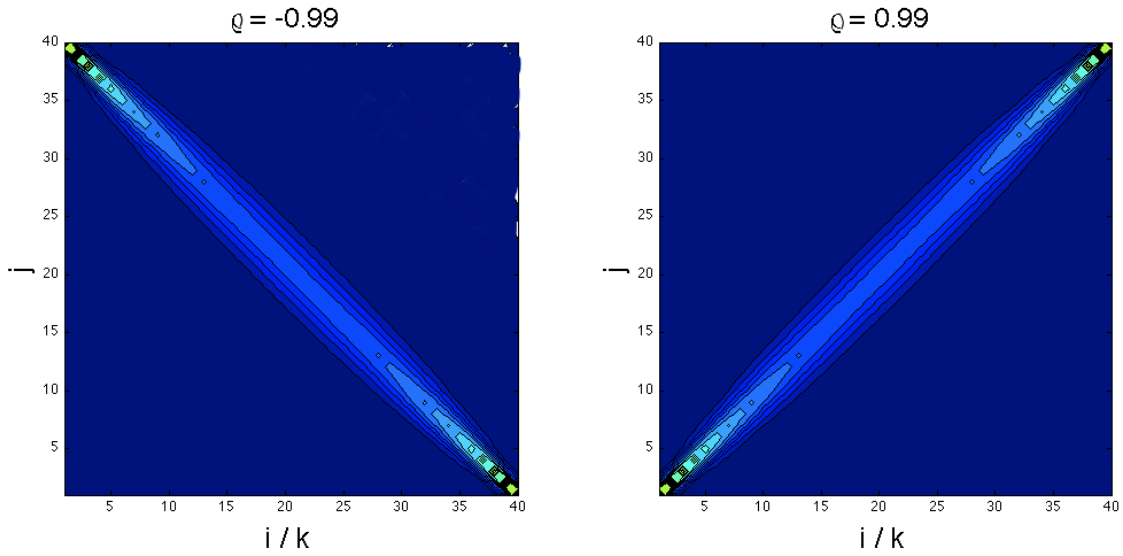

Figure 2.2: Example joint degree distributions for different correlation coefficients

Contour plots of a joint degree distributions generated in this manner are shown in Figure 2.2 for negative and positive values of the correlation coefficient ρ. Because $P_{node}(i,j)$ and $P_{edge}(k,j)$ are found from their respective correlation coefficients ρ_{node} and ρ_{edge} in the same way, the joint distributions shown in Figure 2.2 could be either. An example of the uncorrelated case ($\rho = 0$) is not shown, but would just be a uniform distribution.

These probability distributions can be used to generate degree sequences for realizable networks with the given correlation coefficient. However, the simulation method we employ does not require we generate actual realizations of directed graphs. Rather, it is sufficient to calculate the probability that one of the i incoming connection to a neuron with in-degree i and out-degree j comes from a neuron with in-degree k and out-degree l. This probability, $P(k,l|i,j)$ can be calculated from the joint degree distributions $P_{node}(i,j)$ and $P_{edge}(k,j)$ as follows:

$$P(k,l|i,j) = \frac{lP_{node}(k,l)}{\sum_l lP_{node}(k,l)} \frac{P_{edge}(k,j)}{\sum_k P_{edge}(k,j)}. \tag{2.3}$$

2.2 Excitatory Network with External Stimulation

2.2.1 Integrate-and-Fire Model

The integrate-and-fire model for a neuron has a membrane potential V governed by the current balance equation.

$$C\frac{dV}{dt} = -g_L(V - E_L) - g_{SYN}(V - E_{SYN}) \tag{2.4}$$

where C is the membrane capacitance, g_L and g_{SYN} are the the leak and synaptic conductances, and E_L and E_{SYN} are the leak and synaptic reversal potentials. Whenever the membrane potential crosses a threshold V_θ, the neuron "fires" and the membrane potential instantaneously returns to V_{reset}.

The above parameters are constants except for the synaptic conductance g_{SYN}. The synaptic conductance increases when presynaptic neurons fire and decays to zero in the absence of presynaptic stimulation. The time evolution of the synaptic conductance is governed by

$$\frac{dg_{SYN}}{dt} = -\frac{g_{SYN}}{\tau_g} + \gamma\nu, \tag{2.5}$$

where the conductance time constant τ_g governs the conductance's decay, γ is the strength of synaptic connections, and ν is the total presynaptic firing rate.

2.2.2 Population-Density Model

We are interested in large populations of neurons. Each neuron in a population could be modeled by an integrate-and-fire equation, but the number of equations required would be intractable. Cai et al. developed a probabilistic approach to this problem, starting by interpreting ν as a Poisson process [2]. From this interpretation we can obtain a function for the probability that a neuron randomly sampled from a large network has voltage v and conductance g at time t [1],

$$p(v, g_{syn}, t) = \mathbb{E}[\delta(v - V_i(t))\delta(g_{syn} - G_i(t))]. \tag{2.6}$$

This equation can be differentiated to give a partial differential equation governing the time-evolution of the probability distribution $p(v, g_{syn}, t)$. The resulting PDE, as presented in prior work (reference [1]), aassumed a large random network with a specified in-degree distribution. Modifying that PDE to include possible correlations of in-degree i and an out-degree j gives

$$\begin{aligned}\frac{\partial}{\partial t}p_{i,j}(v, g_{SYN}, t) = \frac{\partial}{\partial v}\left[\left(\left(\frac{v - V_{reset}}{\tau}\right) + g_{SYN}\left(\frac{v - V_\theta}{\tau}\right)\right)p_{i,j}(v, g_{SYN})\right] + \\ \frac{\partial}{\partial g_{SYN}}\left[\frac{1}{\tau_g}\left((g_{SYN} - \bar{g}_{SYNi,j}(t)) + \sigma^2_{g_{SYN},i,j}(t)\frac{\partial}{\partial g}\right)p_{i,j}(v, g, t)\right]\end{aligned} \tag{2.7}$$

$$\bar{g}_{SYNi,j}(t) = f\nu_{0,i,j} + Si\mu_{i,j}(t) \tag{2.8}$$

$$\sigma^2_{g,i,j}(t) = \frac{1}{2\tau_g}\left[f^2 v_{0,i,j} + S^2 i\mu_{i,j}(t)\right] \tag{2.9}$$

where v is the membrane potential , V_{reset} is the reset potential, E_{SYN} is the excitatory current reversal potential, $\sigma^2_{g_{SYN},i,j}$ is conductance variance of neurons in subpopulation i, j, g_{SYN} is the synaptic conductance , $\bar{g}_{i,j}$ is the mean conductance of i, j neurons, S is the connection strength between neurons, and $\mu_{i,j}$ is the average firing rate seen by a neuron of in-degree i and out-degree j.

The "mean-field limit" can be used when the number of neurons in each subpopulation $N \to \infty$, the frequency of stimulation $f \to 0$, the rate at which external stimulation increases synaptic conductance $\xi \to$ a constant, and V and g are uncorrelated. Under these conditions, equation 2.7 reduces to a simpler form where the mean conductance is governed

by the following ODE.

$$\frac{\partial}{\partial t}p_{i,j}(v, g_{SYN}, t) = \frac{\partial}{\partial v}\left[\left(\left(\frac{v - V_{reset}}{\tau}\right) + g_{SYN}\left(\frac{v - E_{SYN}}{\tau}\right)\right)p_{i,j}(v, g_{SYN}, t)\right] + \frac{\partial}{\partial g_{SYN}}\left[\frac{1}{\tau_g}\left(\left(g_{SYN} - \bar{g}_{i,j}(t)\right)\right)p_{i,j}(v, g_{SYN}, t)\right] \tag{2.10}$$

$$\frac{d}{dt}\langle g_{SYNi,j}\rangle = -\frac{1}{\tau_g}\langle g_{SYNi,j}\rangle + g_{S\bar{Y}Ni,j}(t) \tag{2.11}$$

Using the conservation condition

$$\frac{d}{dt}p_{i,j}(v) + \frac{d}{dv}J_{i,j,V}(v) = 0 \tag{2.12}$$

we can find $J_{i,j,V}$, the flux of p through the voltage V. For $V = V_\theta$ this is the firing rate

$$m^{ij} = \left[\tau_{REF} + \frac{C}{g_L + g_{SYN}}\ln\left(\frac{\left(E_L - E_{SYN}\right)g^{ij}_{SYN}}{\left(E_T - E_{SYN}\right)g^{ij}_{SYN} + \left(E_T - E_L\right)g_L}\right)\right]^{-1} \tag{2.13}$$

for $g^{ij}_{SYN} > g_L\left(E_T - E_L\right)/\left(E_{SYN} - E_T\right)$ and $m^{ij} = 0$ otherwise. In this expression C is the membrane capacitance, g_L is the leak conductance, E_L is the leak reversal potential, g_{SYN} is the synaptic conductance, and E_{SYN} is the synaptic reversal potential.

Substituting $\bar{g}_{i,j}$ into equation 2.11 gives the ODE governing the synaptic conductance g_{SYN},

$$\frac{dg^{ij}_{SYN}}{dt} = -\frac{g^{ij}_{SYN}}{\tau_g} + \xi + iS\sum_{k,l}P(k, l|i, j)m_{kl} \tag{2.14}$$

where S is the coupling strength of neurons within the group, ξ is the external stimulation from neurons outside the group, and $P(k, l|i, j)$ is the probability that one of a neuron with in-degree i and out-degree j's incoming connections comes from a neuron with in-degree k and out-degree l. (See equation 2.3 on page 6).

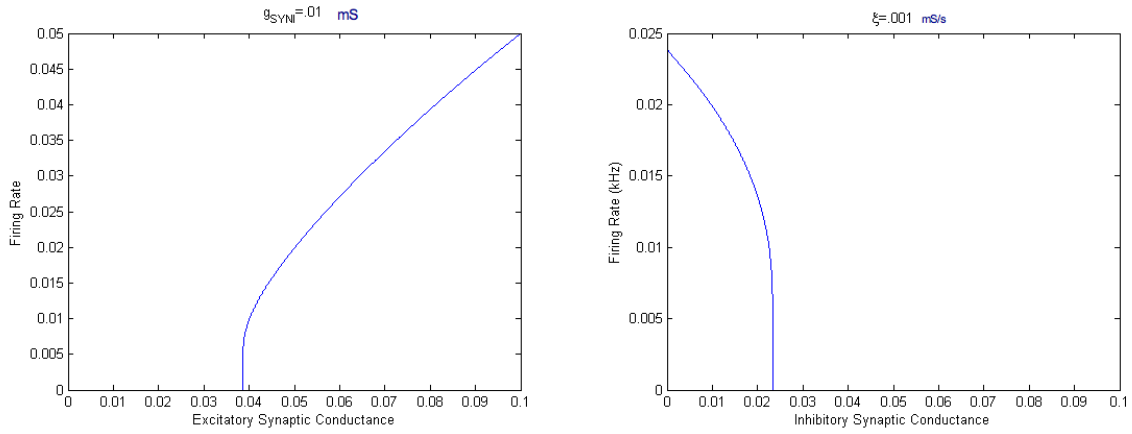

Figure 2.3: Plot of the conductance-frequency relationships given in equation 17

2.3 Externally-Driven Inhibitory Network

With a few simple changes to the conductance and voltage equations, the model we use for an excitatory network can be extended to model an inhibitory network with external excitatory stimulation (see equation 2.14 on the preceding page). The membrane voltage of the inhibitory neurons is still given by an integrate-and-fire model. However, the model includes two synaptic currents because the neurons receive both excitatory and inhibitory stimulation.

$$C\frac{dV^{ij}}{dt} = -g_L\left(V^{ij} - E_L\right) - g_{SYNI}^{ij}\left(V^{ij} - E_{SYNI}\right) - g_{SYNE}\left(V^{ij} - E_{SYNE}\right) \quad (2.15)$$

A difference between the reversal potentials E_{SYNI} and E_{SYNE} accounts for the difference in effect of the two currents. The firing rate m^{ij} for this version of the model is given by making the substitutions $E_L = \frac{g_L E_L + g_{SYNI}^{ij} E_{SYNI}}{g_L + g_{SYNI}^{ij}}$ and $g_L = g_L + g_{SYNI}^{ij}$ in equation 2.13 on the previous page. This conductance-frequency relation is plotted in figure 2.3. When the network is subjected to constant external stimulation, the excitatory synaptic conductance remains constant ($g_{SYNE} = \tau_G \xi$). The inhibitory synaptic conductance dynamics are given

by

$$\frac{dg_{SYNI}^{ij}}{dt} = -\frac{g_{SYN}^{ij}}{\tau_g} + iS\sum_{k,l} P_r(k,l|i,j)m_{kl}, \tag{2.16}$$

similar to equation 2.14 on page 9.

2.4 Numerical Methods

2.4.1 Steady-State Firing Rates

The differential equations for conductance (equation 2.14 on page 9 for the excitatory network and equation 2.16 for the inhibitory network) are numerically integrated starting from both a high and a low initial conductance using MATLAB's built-in function, ode45. At regular intervals, the mean firing rate is compared to the previous mean firing rate in order to determine if it has relaxed to a steady-state value, at which point the steady-state mean firing rate is recorded. In extensive parameter studies run on the SciClone cluster, this method is repeated to find the high and low steady-state firing rates for different values of ξ, S, ρ_N and ρ_E.

2.5 Parameters

Parameter Values		
Parameter	Symbol	Value
Refractory Period	τ_{REF}	4 ms
Membrane Capacitance	C	2.1 μF
Leak Conductance	g_L	0.035 mS
Conductance Time Constant	τ_G	50 ms
Leak Reversal Potential	E_L	–65 mV
Excitatory Synaptic Reversal Potential	E_{SYN} and E_{SYNE}	0 mV
Inhibitory Synaptic Reversal Potential	E_{SYNI}	–65 mV
Threshold Voltage	E_T	–35 mV
External Stimulation	ξ	.00001 to .001 mS/s
Coupling Strength	S	.000036 to .1 mS
Node-Degree Correlation	ρ_{node}	–.99 to .99
Edge-Degree Correlation	ρ_{edge}	–.99 to .99

Standard values for the integrate-fire-and-burst model follow reference [5]. Physiologically appropriate values for ξ and S, ρ_{node}, and ρ_{edge} could vary and ranges for these variables are selected based on system behavior.

Chapter 3

Results

3.1 Effect of Node-Degree Correlations on Mean Firing Rate

In an excitatory network, increasing the node-degree correlation and edge-degree correlation results in a slight increase in the mean-firing rate of the network (see Figure 3.1 on the following page.) This result is unsurprising because neurons with high in-degree receive the most stimulation and thus fire more frequently. In a strongly correlated network, the neurons with the highest firing rate are also the neurons with the most outgoing connections. This confluence achieves the maximum stimulation of post-synaptic neurons in the network. For inhibitory networks, the same effect is observed, because the most inhibited neurons are those who inhibit the most other neurons when they fire. For both inhibitory and excitatory networks, the node-degree correlation has a noticeably stronger effect than the edge-degree correlation.

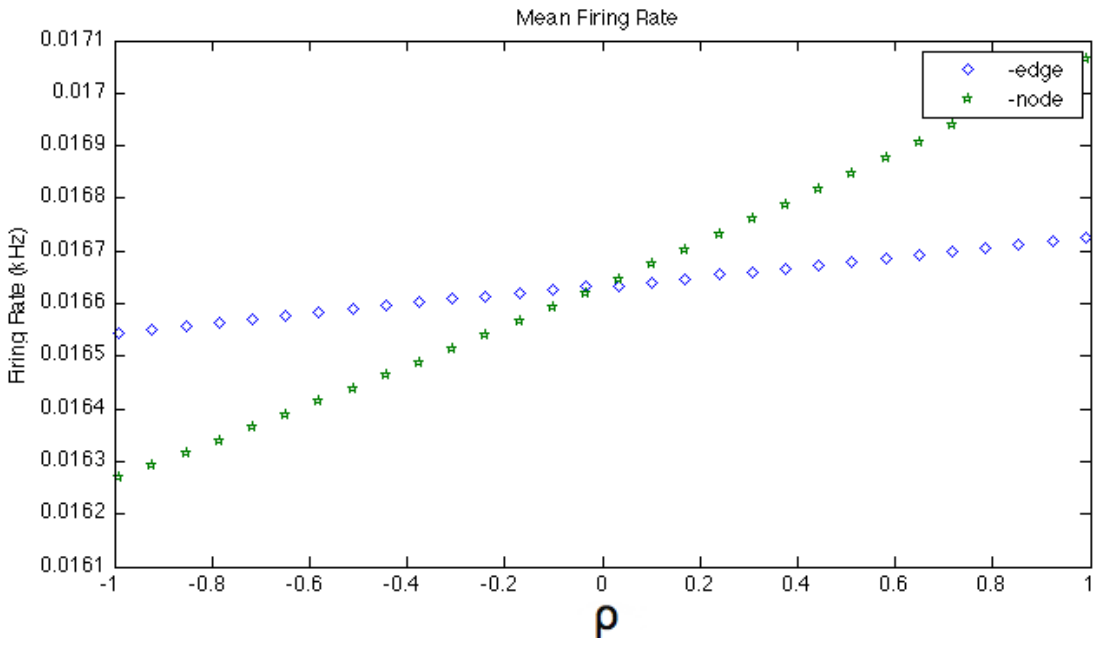

Figure 3.1: Mean firing rate at steady-state for an excitatory network shown as a function of the correlation coefficients. Each is a monotonically increasing function with little dependence on the correlation coefficients.

3.2 External Stimulation and Hysteresis

Figure 3.2 on the next page confirms this model is capable of exhibiting hysteresis. At low external stimulation rates, there is only a single quiescent state. For intermediate external stimulation rates, there are two steady-state firing rates, one quiescent and one active. If the external stimulation rate increases above a certain threshold, only the active state remains. In the intermediate region, the network remains in the active state if external stimulation was previously high and in the quiescent state if external stimulation was previously low.

Note that although the quiescent state appears completely inactive, the corresponding physical system would have a small nonzero firing rate. This is because the mean-driven limit used here does not account for fluctuation-driven neural activity. Near the discontinuity in the firing rate function the current-frequency relation for the mean-driven limit differs significantly from the behavior of less reduced models such as monte carlo simulation of

integrate-and-fire neurons or the population density model (equation 2.7) [2].

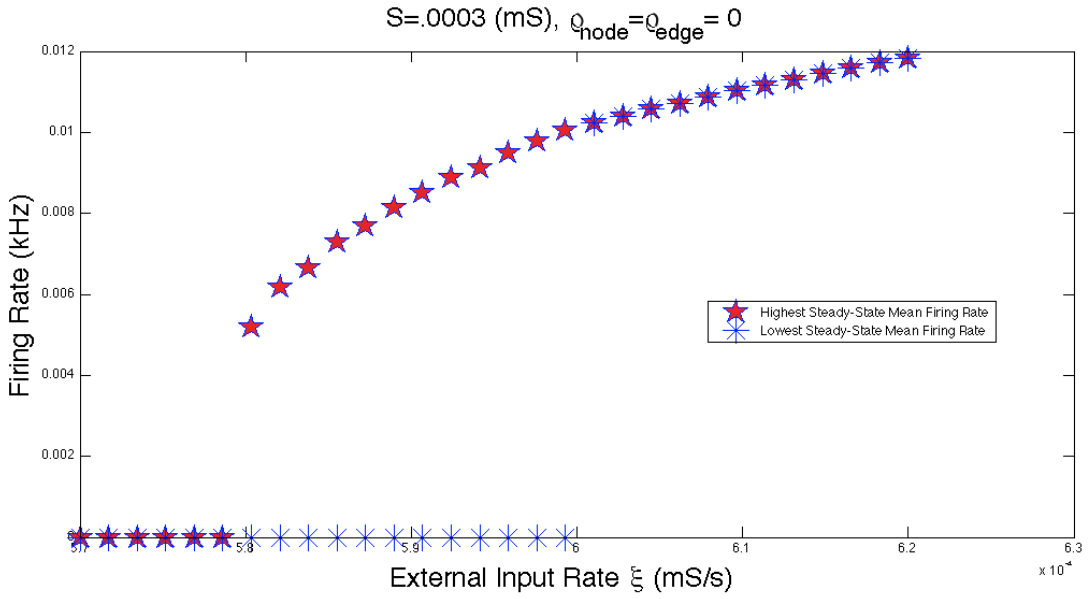

Figure 3.2: Steady-state firing rate for different external input rates.

3.3 Effect of Node-Degree and Edge-Degree Correlation on Hysteresis

Both node-degree correlation and edge-degree correlation have the same general effects on hysteresis. Figure 3.3 on the following page shows parameter studies over coupling strength and external stimulation rate for different combinations of ρ_{node} and ρ_{edge}. In an excitatory network, when the network is highly correlated, the range of external stimulation rates with bistable steady-state firing rates increases. When the network is strongly anti-correlated, this range decreases. However, when the network is strongly correlated, the range of coupling strengths where low external stimulation allows only the quiescent steady state to exist decreases. For anti-correlated networks, this range increases.

The threshold value of external stimulation above which only the active state exists

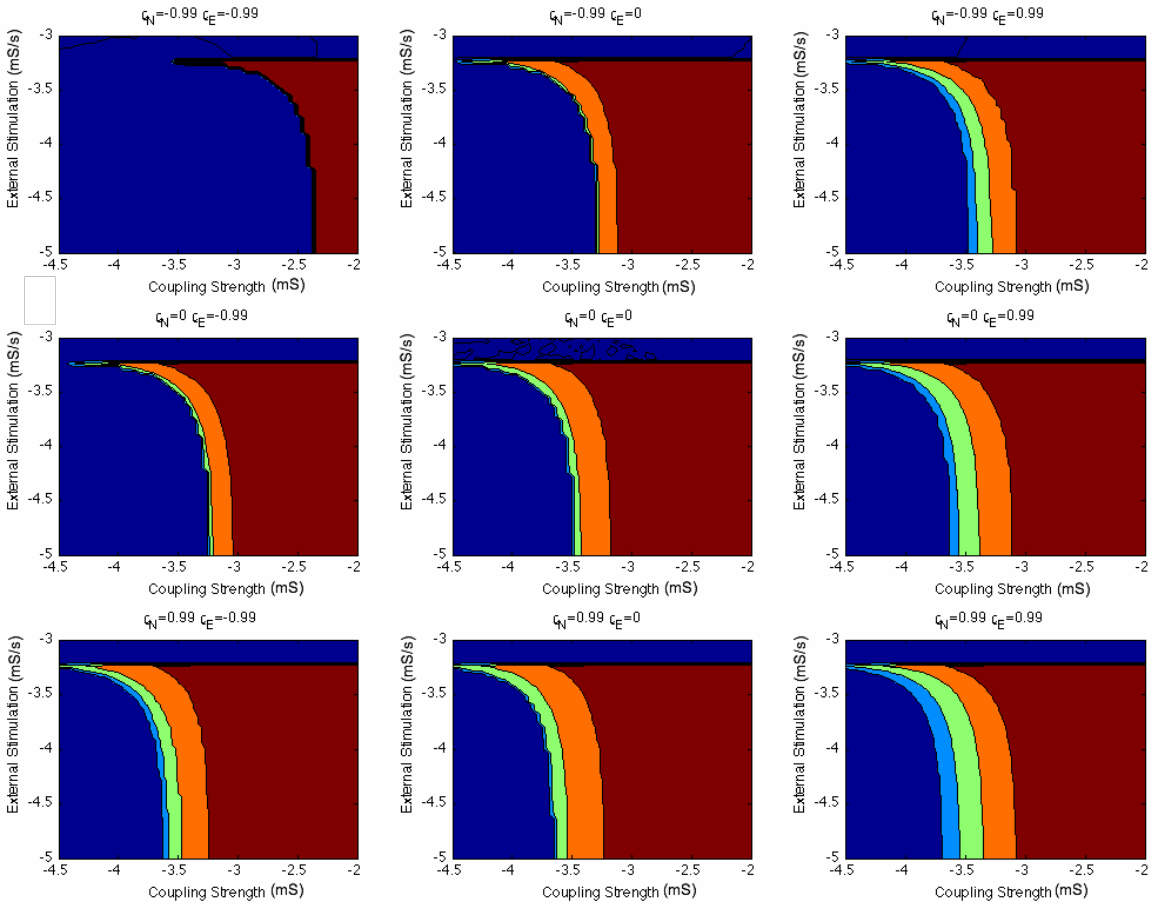

Figure 3.3: Parameter-scans over external stimulation rate and coupling strength at different values of the correlation coefficient. Blue indicates the presence of one steady-state firing rate, with other colors representing a separation between low and high steady-states with red being the maximum separation between them. In the lower-left blue region, only the quiescent steady state exists while in the uppermost blue region only the active steady state exists. Blue corresponds to a difference of 0-50 Hz, sky blue to 50-100 Hz, green to 100-150 Hz , orange to 150-200 Hz, and red to a difference of 200-250 Hz

is not sensitive to changes in either coupling strength or node or edge-degree correlation. This contradicts our expectation that the threshold value should decrease for higher S, ρ_{node}, or ρ_{degree}. The absence of any effect may be due to the discontinuity in the firing rate expression used in this model.

Figure 3.3 also suggests that the more anti-correlated the network, the sharper the onset of hysteresis as coupling strength is increased. To explore this phenomenon, the mean

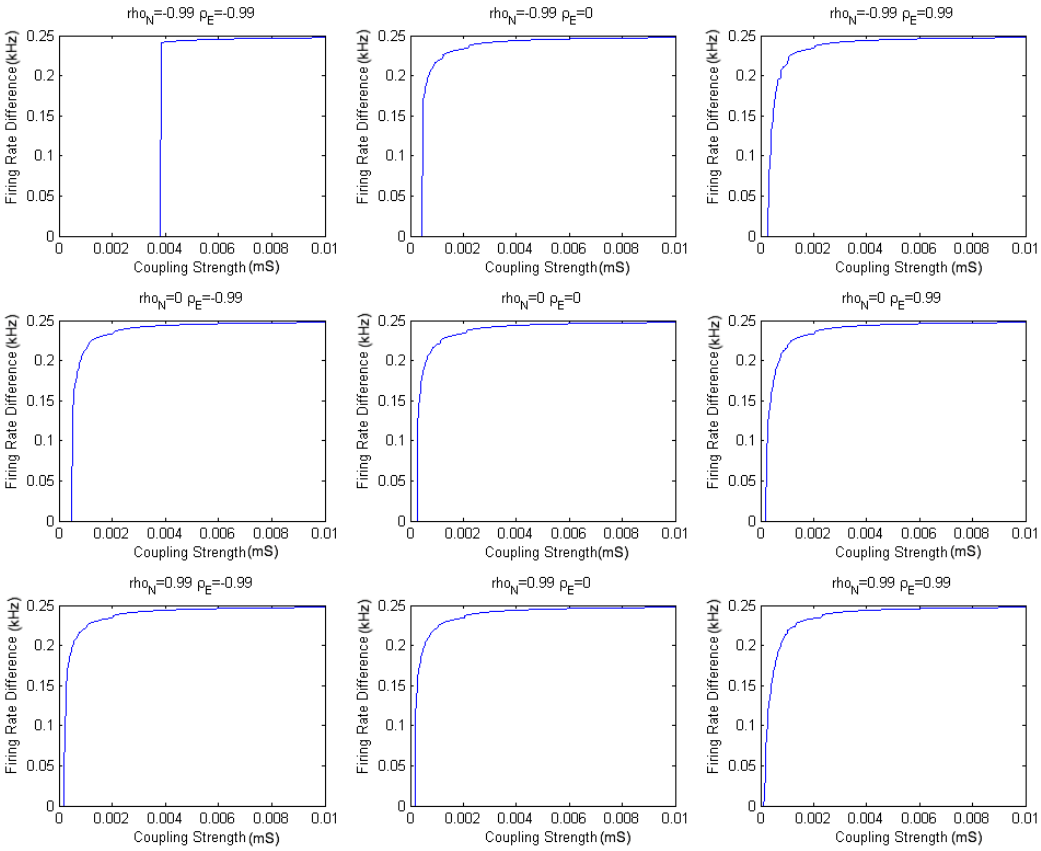

Figure 3.4: Parameter studies of the highest steady-state firing rates are show for different node-degree correlations (increasing top to bottom) and different edge-degree correlations (increasing from right to left.)

firing rate as a function of coupling strength with fixed external stimulation is plotted in Figure 3.4 and Figure 3.5 on the next page. The results suggest both node and edge-degree anti-correlation makes the transition sharper. Furthermore, when both node-degree and edge-degree are strongly anti-correlated, the transition is much sharper than one would expect from either alone.

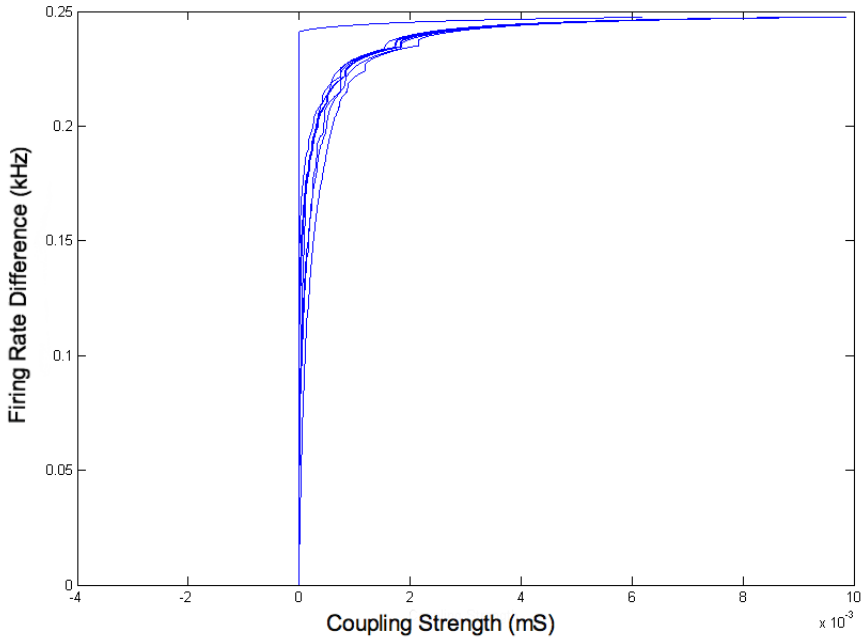

Figure 3.5: The highest steady state firing rates, overlaid and shifted left so that the appearance of the active steady-state firing rate occurs at the same value of S. The almost instantaneous transition occurs when node-degree and edge-degree are both anti-correlated.

3.4 Hysteresis in a Driven Inhibitory Network

Calculations took significantly longer for the driven inhibitory network, and for some parameter values the numerical solutions would not converge. This problem occurred most often when simulating positively correlated networks. Figure 3.6 on the following page shows how external stimulation and coupling strength affect hysteresis in an anti-correlated and uncorrelated network. These results suggest increasing the node-degree correlation allows bistability over a greater range of coupling strengths. Increasing the correlations also "flattens out" the external stimulation threshold for bistability, reducing the threshold values dependence on coupling strength.

Figure 3.7 on page 20 shows the equivalent parameter study for a positively correlated network. The positively correlated network appears to be more similar to the uncorrelated

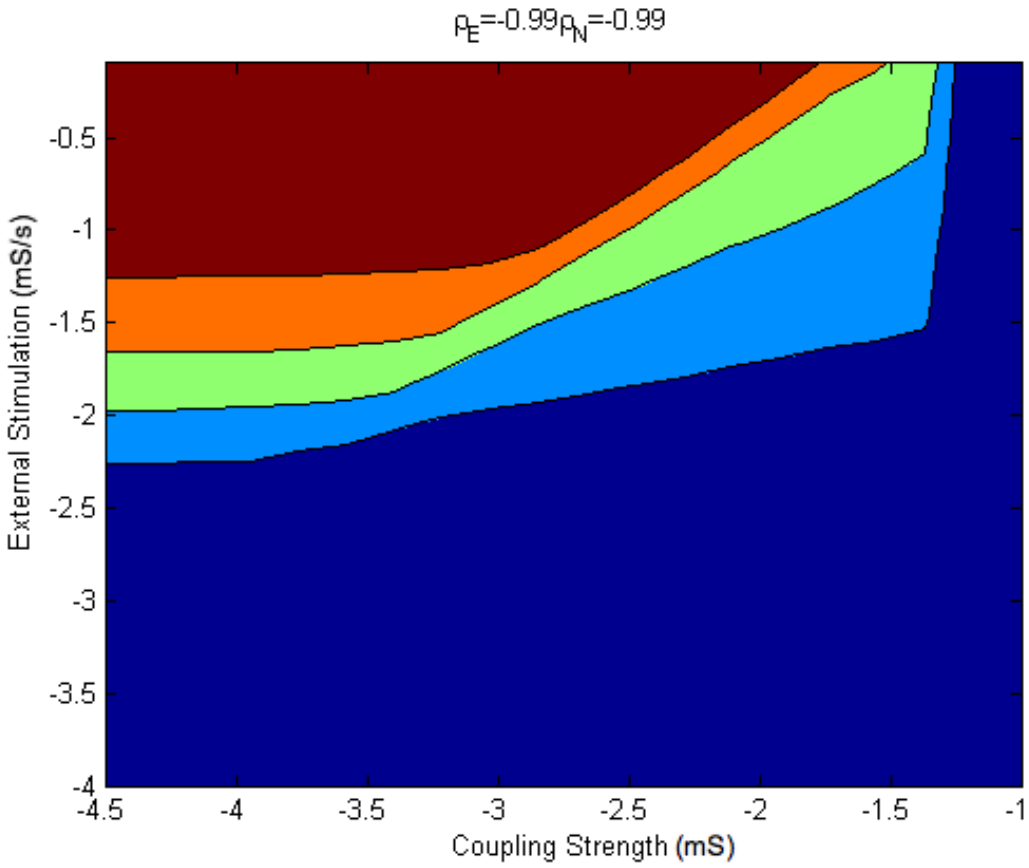
ρ_E=-0.99ρ_N=-0.99
External Stimulation (mS/s)
-0.5
-1
-1.5
-2
-2.5
-3
-3.5
-4
-4.5
-4
-3.5
-3
-2.5
-2
-1.5
-1
Coupling Strength (mS)

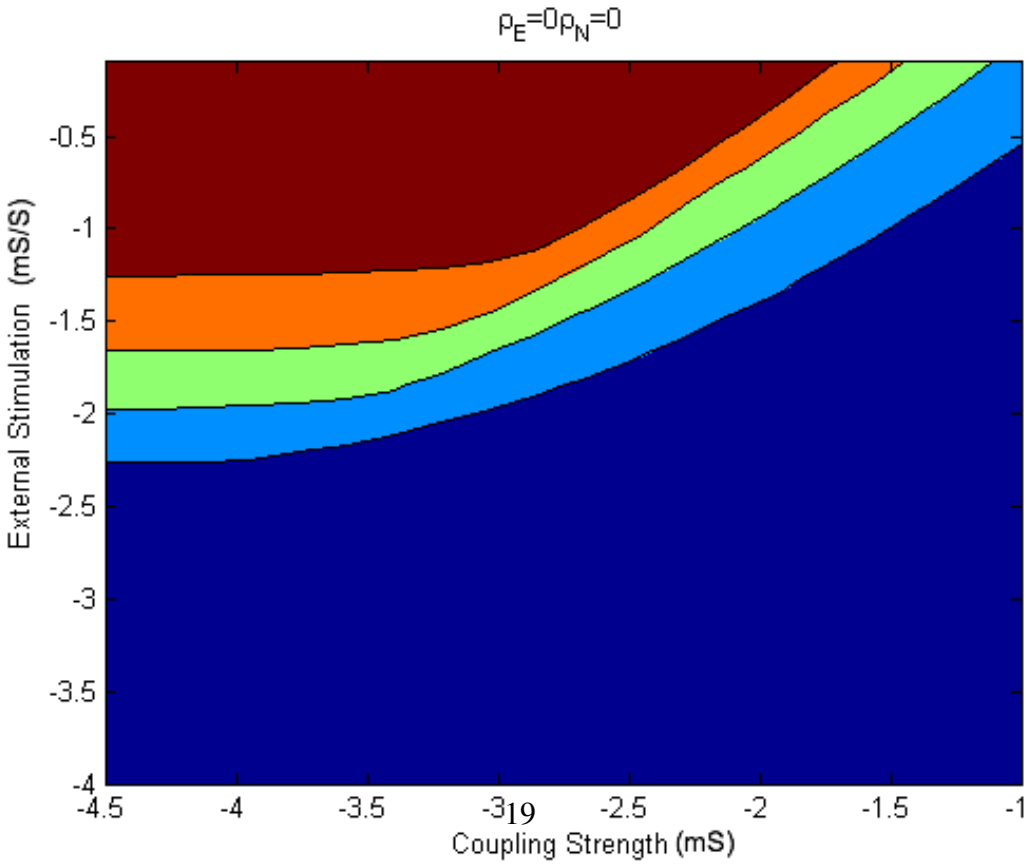
ρ_E=0ρ_N=0
External Stimulation (mS/S)
-0.5
-1
-1.5
-2
-2.5
-3
-3.5
-4
-4.5
-4
-3.5
-3
-2.5
-2
-1.5
-1
Coupling Strength (mS)

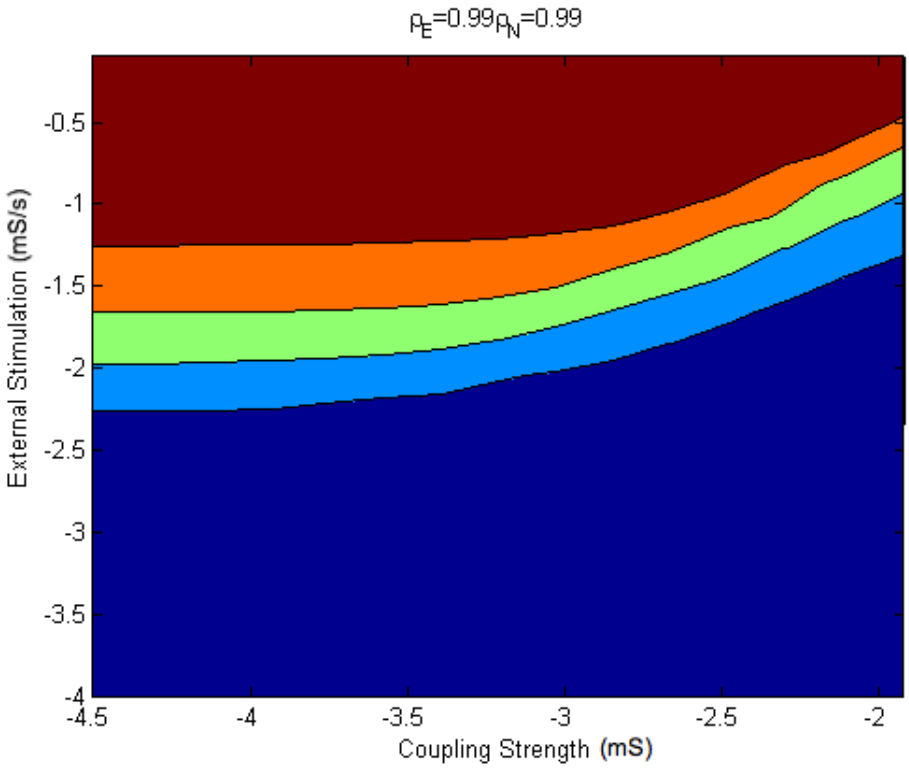

Figure 3.7: Parameter dependence of hysteresis in an externally driven inhibitory network with positive node-degree and edge-degree correlation. Color-coding correspond as in Figure 3.6.

network than the uncorrelated network is to the anti-correlated network, at least to the extent that we were able to obtain numerical solutions of the governing equations.

Chapter 4

Conclusions

Hysteresis in cortical networks is one proposed explanation for the synaptic reverberation underlying working memory. Using a mean-field limit version of Cai's population density model extended to incorporate in-and-out degrees, this investigation studied how node- and edge-degree correlations affected hysteresis of network activity. The results of these simulations suggest that node-degree correlation and edge-degree correlation can impact the parameter-dependence of bistability. Strongly anti-correlated networks allow a wide-range of coupling strengths where the quiescent state can exist on its own. This would allow a sudden drop in external stimulation or temporary inhibitory input to move the network to its quiescent state until the network is again stimulated. Anti-correlated networks also create a sharper transition to hysteresis as coupling strength is changed, allowing a sharper signal. Strongly correlated networks, on the other hand, allow a more graded response (perhaps important if the information encoded is not binary) and also broaden the range of hysteresis at low coupling strength values.

Altogether, these results suggest node-degree correlation and edge-degree correlation are physiologically relevant aspects of network architecture. As new techniques for tracking neuronal connections are developed, more detailed knowledge of in-and-out degree correlation of cortical networks will become available.

Future theoretical work in this area would also be helpful. This study pushes the mean-driven limit model to its limits. Numerical instability encountered while attempting to simulate the inhibitory network is probably due to the discontinuous derivative of the firing rate expression for integrate and fire neurons (see Figure 2.3 on page 10). Performing additional simulations to study the effect of degree correlations using the full population density model (or reductions that account for the presence of nodes with unusually high conductance) would provide a more complete picture of the behavior of inhibitory networks. It should also be noted that the node-degree and edge-degree correlation studied here are only two of many possible degree-correlations. Studying other degree correlations could reveal their physiological relevance.

Acknowledgements

I would like to thank my advisor, Greg Smith, for his guidance on this project; without which I would not have overcome the many roadblocks I stumbled on. I am also very grateful to Drew Lamar, who provided his invaluable knowledge of networks and lots of Matlab help. Funding for work on this project was provided by CSUMS and the Charles Center, while SciClone provided the computing power I needed for the extensive parameter studies performed.

Bibliography

[1] David Cai. Fluctuations in neuronal network dynamics. In *Joint Mathematics Meeting Session on Stochastic Processes in Neuroscience*, 2011.

[2] David Cai, Louis Tao, David Mclaughlin, and Aaditya Rangan. Kinetic theory for neuronal network dynamics. *Comm. Math. Sci.*, 4(1):97–127, 2006.

[3] M. D. Lamar and G. D. Smith. Effect of node-degree correlation on synchronization of identical pulse-coupled oscillators. *Physical Review E*, 81(4):046206:1–11, April 2010.

[4] M. S. Shkarayev, G. Kovacic, A.V. Rangan, and D. Cai. Architectural and functional connectivity in scale-free integrate-and-fire networks. *Europhysics Letters*, 88(5), December 2009.

[5] Gregory D. Smith, Charles L. Cox, S. Murray Sherman, and John Rinzel. Fourier analysis of sinuisodially driven thalamocortical relay neurons and a minimal integrate-and-fire-or-burst model. *Journal of Neurophysiology*, 83(1):588–610, 2000.

[6] Olaf Sporns. *Networks of the Brain*. The MIT Press, 2011.

[7] X. Wang. Synaptic reverberation underlying mnemonic persistent activity. *TRENDS in Neurosciences*, 24(8):455–463, August 2001.